Field Emission Tip as a Nanometer Source of Free Electron Femtosecond Pulses

Peter Hommelhoff,* Yvan Sortais, Anoush Aghajani-Talesh, and Mark A. Kasevich
Physics Department, Stanford University, Stanford, California 94305, USA
(Received 25 July 2005; published 21 February 2006)

We report a source of free electron pulses based on a field emission tip irradiated by a low-power femtosecond laser. The electron pulses are shorter than 70 fs and originate from a tip with an emission area diameter down to 2 nm. Depending on the operating regime we observe either photofield emission or optical field emission with up to 200 electrons per pulse at a repetition rate of 1 GHz. This pulsed electron emitter, triggered by a femtosecond oscillator, could serve as an efficient source for time-resolved electron interferometry, for time-resolved nanometric imaging and for synchrotrons.

DOI: 10.1103/PhysRevLett.96.077401 PACS numbers: 78.47.+p, 41.75.−i, 79.70.+q

Continuous electron sources based on field emission can have emission areas down to the size of a single atom. Such spatially resolved sources have stunning applications in surface microscopy, to the extent that atomic-scale images of surfaces are commonplace [1,2]. Because of their brightness, field emission electron sources are also enabling for electron interferometry. Recently, for example, such small tips have been used to demonstrate antibunching of free electrons in a Hanbury Brown–Twiss experiment [3].

On the other hand, the recent development of ultrafast pulsed electron sources has enabled time-resolved characterization of processes on atomic time scales. For example, the melting of a metal has been observed with 600 fs electron pulses [4]. Subfemtosecond electron pulses have been used to study the ionization dynamics of H_2 [5]. Fast electron pulses are typically generated by focusing an amplified high-power femtosecond laser beam onto a photocathode [6] or a vapor target. In this case, the electron emission area is given by the laser spot diameter, which is on the order of or larger than 1 μm, much larger than the emission area for continuous sources.

Emerging applications, such as ultrafast electron microscopy [7], will require complete control over the spatiotemporal characteristics of the emitted electrons. In this Letter we realize this control through use of a low-power femtosecond laser oscillator to trigger free electron pulses from sharp field emission sources. Sharp tips and femtosecond lasers have previously been combined in the context of time-resolved scanning tunneling microscopy [8–10].

For weak optical fields, photoemission is dominated by the photofield effect [11], in which an initially bound electron is promoted in energy by $\hbar\omega$ through absorption of a single photon of frequency ω and subsequently tunnels to the continuum [Fig. 1(a)]. Because of the physical characteristics of the tunneling process, electron emission is prompt with respect to the incident electric field. For stronger optical fields, the local electric field associated with the optical field directly modifies the tunneling potential [optical field emission, Fig. 1(b)], again leading to prompt electron emission. We are able to continuously tune between the photofield and optical field emission regimes by varying the intensity of the driving laser. These prompt mechanisms compete with thermally induced emission, which takes place on time scales of tens of femtoseconds to picoseconds [12–14]. We are able to find operating conditions where the thermal mechanisms are negligible.

In our experiment, the output from a Kerr-lens modelocked Ti:sapphire laser is focused on a field emission tip (Fig. 2). The laser operates at a 1 GHz repetition rate, and produces a train of 48 fs pulses (measured with an interferometric autocorrelator) at a center wavelength of $\lambda \sim 810$ nm with maximum average power of 600 mW. The field emission tip is made of electrochemically etched 0.125 mm diameter tungsten single crystal wire in the (111) orientation. The tip is mounted in an ultrahigh vacuum chamber and faces a microchannel plate detector (MCP) located 4 cm away from the tip. Field emitted electrons are accelerated onto the MCP detector. The amplified output is proximity focused on a phosphor screen. A CCD camera records the resulting image, which reflects

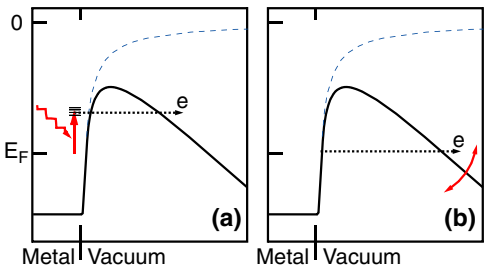

FIG. 1 (color online). Photofield emission (a) and optical field emission (b) energy diagrams. In photofield emission an electron is excited by a laser photon to an intermediate state and then tunnels through the barrier, which is generated by a dc voltage applied to the tip. In optical field emission, the laser field instantaneously wiggles the barrier. If the barrier is sufficiently thin, electrons tunnel from the Fermi level. This process is dominant for high fields. Dashed line: no field applied on the tip.

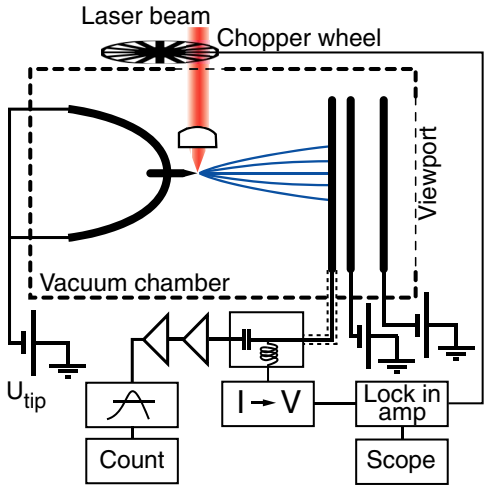

FIG. 2 (color online). Experimental configuration, see text for details.

the spatial distribution of photoelectrons. The time of arrival of amplified photoelectrons is obtained by monitoring the MCP bias current. At high MCP gains, we obtain spatial and temporal single electron detection resolution.

The local electric field strength at the tip is determined by the laser beam parameters (spot size, power, pulse duration, and polarization), and local field enhancements due to plasmon resonances and lightening rod effects [see, for example, [15]]. We focus the laser output to a 3 μm spot size ($1/e^2$ radius) at the tip with an aspheric lens mounted within the vacuum chamber. The propagation vector of the laser beam is perpendicular to the tip shank, and an achromatic half wave plate outside the chamber is used to control the beam's polarization. We estimate that the focusing lens ($f = 7.5$ mm) stretches the pulses to approximately 65 fs in the focus [see [16,17]], so that the peak intensity at the tip is 3×10^{10} W/cm^2. For tungsten, the plasmon enhancements are relatively weak, while the lightening rod enhancement is $\sim$5 for a tip with a radius of curvature $r < \lambda/5$ [15]. Thus, we estimate the maximum electric field at the tip to be in excess of 1 GV/m.

To experimentally determine the relevant emission mechanism, and, in particular, to demonstrate that electron emission is prompt with respect to the incident field, we studied emission characteristics as a function of the dc bias voltage, laser intensity, and laser polarization. Figure 3 shows emission data taken with a $r = 130$ nm tip in the photofield regime. In Fig. 3(a) we measure the emitted current I as a function of the tip bias voltage U, both with and without the laser illumination. In both cases, data are fit to the Fowler-Nordheim equation [18], which relates the tunnel current density j to the local electric field strength F and the effective work function Φ:

$$j = \frac{e^3 F^2}{8\pi h \Phi t^2(w)} \exp\left[-\frac{8\pi\sqrt{2m}\Phi^{3/2}}{3heF} v(w) \right]. \quad (1)$$

Here, e is the electron charge, h Planck's constant, m the electron mass, $0.4 < v(w) < 0.8$ is a slowly varying function taking into account the image force of the tunneling electron, $t^2(w) \approx 1$ for field emission, and $w = e^{3/2}\sqrt{F/(4\pi\epsilon_0)}/\Phi$. F is determined through $F = U/(kr)$ with $k = 5.7$ [19]. The electron current I is related to the current density through $I = 2\pi R^2 j$, with R the radius of the emitter area.

We compare emission data with and without laser illumination to show that, for low power, electrons are emitted through photofield emission. We use the measurements without illumination and the known work function of tungsten to infer the tip radius r. Since r does not change under laser illumination, we can then use this value to determine the effective work function when the tip is illuminated with the laser. We deduce that the effective work function is reduced by 1.5 eV under illumination, which corresponds to the energy of the absorbed 810 nm laser photon. We verified that the value of the inferred effective work function was insensitive to laser power for low laser power. This is reflected in the observed linear dependence of photo current on incident laser power, as shown in Fig. 3(d).

Further supporting evidence for photofield emission is provided by the polarization dependence of the photo current shown in Fig. 3(b). It exhibits a $\cos^2\theta$ behavior, where θ is the angle between the tip shank and polarization vector for the field. This is indicative of optical excitation of surface electrons, since translation symmetry prohibits excitation by the field component parallel to the surface [20]. In stark contrast, for thermally induced field emission one would expect to see a sinusoidally varying photo current that is phase shifted by 90° with respect to the one observed: Fresnel's equations describe that for the given tip geometry and spot diameter the tip is heated less if the light polarization is parallel to the tip shank and therefore, that the current reaches a maximum at $\theta = 90°$ [21]. We observe this dependence in cw laser illumination. Finally, Fig. 3(c) displays the spectrum analysis of the electron current around the laser repetition rate; a 30 dB signal-to-noise ratio peak is evident at the laser repetition rate.

Taken together, these results show that, for these parameters, the processes involved in the electron emission are dominated by photofield emission. Thus we infer that electron emission is prompt with respect to the laser pulse, and rule out possible thermal emission mechanisms associated with laser induced heating of the tip [12–14,21]. For $U_{\text{tip}} > -1300$ V more than 98% of the emitted electrons are photoemitted.

Decreasing the tip radius leads to smaller emission planes, and emission from a single atom is possible [18,22]. Figure 4(a) shows a field ion microscope (FIM) image of a 30 nm tip. The central emission plane is evident, consisting of a ring of 7 atoms and having an effective area

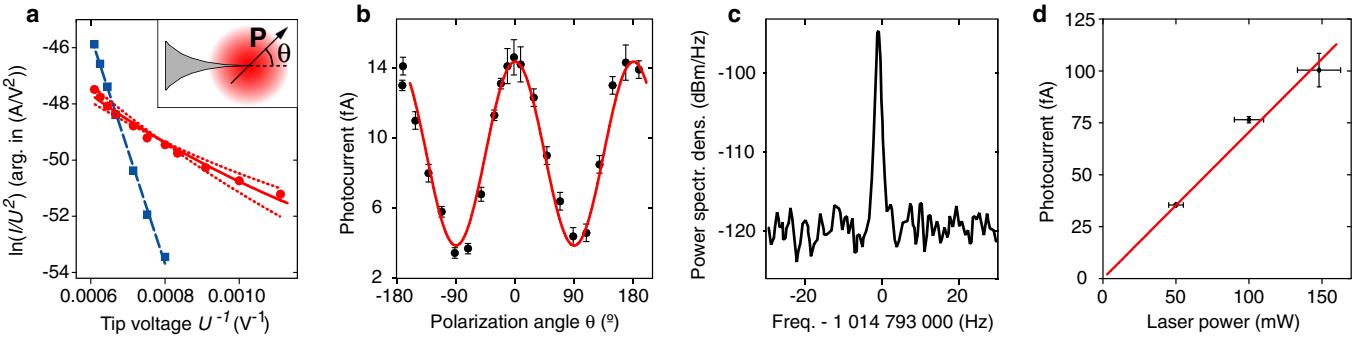

FIG. 3 (color online). Emission for low laser power. (a) Fowler-Nordheim plots of the dc current and the additional photo current (squares and circles). A fit to the dc data (dashed line) yields a tip radius r of (134 ± 3) nm. The solid line is a fit to photofield emission current with $r = 134$ nm and an effective work function $\Phi = \Phi_W - h\nu = 3$ eV (laser power $P = 260$ mW, $\Phi_W = 4.5$ eV). The presence of the laser field F_{laser} at the tip further reduces the barrier in addition to the field due to the dc voltage applied to the tip. Therefore, we leave F_{laser} as a free parameter. The solid red line is drawn with the best fit value of $F_{\text{laser}} = 1.1$ GV/m, and the dotted lines represent a deviation of $\pm 25\%$. With the tip's radius of curvature much smaller than the laser wavelength we expect the laser field to be enhanced at the tip apex by a factor of ~ 5 [15]. By comparing the fitted F_{laser} to the maximum field calculated in the focal spot in the absence of any material, we infer an enhancement factor of 4.1, in good agreement with the expected factor. (b) Polarization dependence of the photocurrent with $U_{\text{tip}} = -1500$ V and $P = 260$ mW for $r = 134$ nm. The data are well fit with a $\cos^2\theta$ on a flat background (red line). The inset in (a) shows the definition of the angle θ (in plane perpendicular to laser propagation direction). (c) 1 GHz repetition rate signal measured in the electron current. The measured linewidth is about 1 Hz at -3 dBc, which corresponds to the resolution limit of the spectrum analyzer. (d) The photo current increases linearly with laser power ($r \approx 40$ nm, $U_{\text{tip}} = -720$ V).

of ~ 2 nm diameter [1]. Figure 4(b) shows the corresponding field emission (FEM) image at low bias voltage, without driving laser pulses. Each grain on the image indicates the detection of an individual electron. Emission from the central atom cluster is the dominant contributor to the photo current. Finally, Fig. 4(c) shows the same tip, at the same bias voltage, illuminated with laser pulses. In this image, the MCP's gain was reduced in order not to saturate the camera. Although the count rate is approximately a factor of 100 higher, the basic structure of the image is unchanged, indicating emission is coming from the sites identified in the FIM and nonilluminated FEM images. In this regime less than one electron is emitted per laser pulse. Because of the smallness of the emission area, such an electron beam is well suited to pulsed interferometer applications [3].

For applications which benefit from higher currents—but not necessarily atomic-scale localization of the emission sites—we investigated emission from blunt tips. Figure 5 displays the polarization dependence of the emission current for a tip that ends in a flat 1 μm radius area, but which still exhibits sharp features for field enhancement [23]. Under 530 mW illumination, time-averaged photo current rises to 40 nA and is, as before, maximal when the field is parallel to the tip. In this case, however, the optical current exhibits a strong nonlinearity in the field component parallel to the tip and can be consistently fit to optical field emission behavior. In this case,

$$j = G(F_{\text{dc}} + F_{\text{laser}}\cos\theta)^2 \exp\left[-\frac{H}{F_{\text{dc}} + F_{\text{laser}}\cos\theta}\right]. \quad (2)$$

Here, F_{laser} is the instantaneous absolute value of the laser field at the tip, F_{dc} the applied dc field, and G and H are constants. This expression is obtained from Eq. (1) by taking the local electric field to be the sum of the dc bias field and the incident laser field. Note that this expression is inherently time dependent due to the presence of F_{laser}. Since we measure the photo current time averaged over more than one optical cycle, we fit the data in Fig. 4 to Eq. (2) with $\cos\theta$ replaced with $|\cos\theta|$, assuming that

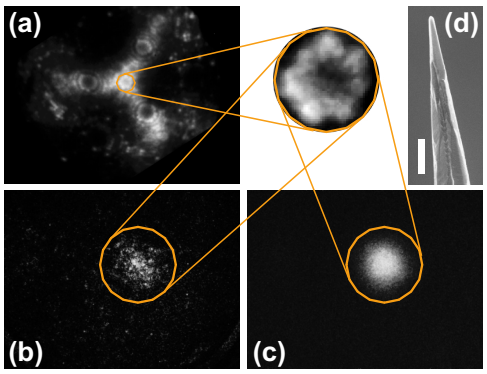

FIG. 4 (color online). Few atom electron source. (a) Field ion microscope image of a 30 nm radius tip. The zoom in reveals the central (111) emission area encircled by a ring of 7 atoms, spanning an area of $\lesssim 2$ nm diameter. (b) dc-field emission image of a 30 nm radius tip; only emission from the central (111) plane is visible, i.e., from the seven atom ring structure in (a). (c) Same tip with laser on, but much smaller (100× reduced) MCP gain than in (b). (d) Scanning electron microscope image (SEM) of a typical tip, scale bar 1 μm.

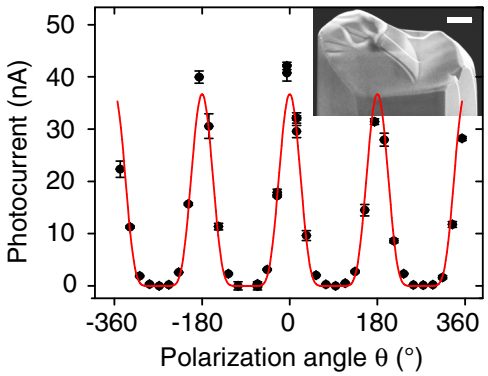

FIG. 5 (color online). Polarization dependence for high laser power. Photocurrent as a function of θ for a stub as shown in the inset (SEM image, scale bar 500 nm). The tip ends as a fairly flat surface facing the MCP. Because of the sharpness of parts of the edges (radius of curvature $\lesssim 100$ nm) field enhancement takes place as for sharp tips ($P = 530$ mW, $U_{\text{tip}} = -100$ V). The line is a fit of the data to optical field emission (see text).

electron emission is dominated by emission at the highest field strengths. Note that due to the exponential dependence of tunneling rate on the applied electric field, even modest intensity changes can dramatically alter emission characteristics. At this high laser power we find that sharper tips ($r < 100$ nm) experience significant redistribution of emitting atoms, by comparing FIM images from before and after tip illumination. On average, about 200 electrons per pulse are drawn from the tip for $\theta = 0$, which corresponds to an instantaneous current of 500 μA or 3.1×10^{15} electrons per second. Assuming the electrons are emitted uniformly over 65 fs and over the entire surface, we can set a lower limit of 15 kA/cm^2 on the instantaneous current density and a lower limit on the invariant brightness of 10^{13} A/(m^{2}sr). Both values are comparable to state-of-the-art electron pulses drawn from photocathodes in synchrotron electron sources [7].

In the future, we envision the techniques demonstrated in this work may lead to generation of sub-1 femtosecond pulses from single-atom tips by exploiting the nonlinearity in the laser-tip interaction [5,24]. Likewise, this nonlinearity might enable a direct measurement of the carrier-envelope phase of the laser pulse [25–28]. Since single-atom tips have been shown to emit electrons via localized states with a lifetime in the range of a few femtoseconds [29,30], tip excitation with laser pulses of a similar or shorter duration in the optical field emission regime may lead to the development of deterministic single electron sources [31], which may have important applications in quantum information science. Finally, optimized nanofabricated tip geometries may lead to sources of unprecedented emission brightness.

We are indebted to Mingchang Liu and Kai Bongs for assistance in the very early stages of this experiment and to Ralph DeVoe and Steve Harris for discussions. This work was supported by the ARO MURI program. P. H. thanks the Humboldt Foundation for financial support and A. A.-T. the DAAD.

*Electronic address: hommelhoff@stanford.edu

[1] T. T. Tsong, *Atom-Probe Field Ion Microscopy* (Cambridge University Press, Cambridge, England, 1990).
[2] *Scanning Tunneling Microscopy II*, edited by R. Wiesendanger, and H.-J. Güntherodt (Springer, New York, 1992).
[3] H. Kiesel, A. Renz, and F. Hasselbach, Nature (London) **418**, 392 (2002).
[4] B. J. Siwick, J. R. Dwyer, R. E. Jordan, and R. J. D. Miller, Science **302**, 1382 (2003).
[5] H. Niikura *et al.*, Nature (London) **417**, 917 (2002).
[6] H. Ihee *et al.*, Science **291**, 458 (2001).
[7] W. E. King *et al.*, J. Appl. Phys. **97**, 111101 (2005).
[8] O. Takeuchi *et al.*, Appl. Phys. Lett. **85**, 3268 (2004).
[9] M. Merschdorf, W. Pfeiffer, A. Thon, and G. Gerber, Appl. Phys. Lett. **81**, 286 (2002).
[10] S. Grafström, J. Appl. Phys. **91**, 1717 (2002).
[11] M. J. G. Lee, Phys. Rev. Lett. **30**, 1193 (1973).
[12] W. S. Fann, R. Storz, H. W. K. Tom, and J. Bokor, Phys. Rev. B **46**, 13 592 (1992).
[13] D. M. Riffe *et al.*, J. Opt. Soc. Am. B **10**, 1424 (1993).
[14] M. Merschdorf, W. Pfeiffer, S. Voll, and G. Gerber, Phys. Rev. B **68**, 155416 (2003).
[15] Y. C. Martin, H. F. Hamann, and H. K. Wickramasinghe, J. Appl. Phys. **89**, 5774 (2001).
[16] M. Kempe, U. Stamm, B. Wilhelmi, and W. Rudolph, J. Opt. Soc. Am. B **9**, 1158 (1992).
[17] Z. I. Horváth and Z. Bor, Opt. Commun. **100**, 6 (1993).
[18] V. T. Binh, N. Garcia, and S. T. Purcell, Adv. Imaging Electron Phys. **95**, 63 (1996).
[19] We determine k through an iterative routine, as described in R. Gomer, *Field Emission and Field Ionization* (Harvard University Press, Cambridge, Massachusetts, 1961).
[20] D. Venus and M. J. G. Lee, Surf. Sci. **125**, 452 (1983).
[21] K. W. Hadley, P. J. Donders, and M. J. G. Lee, J. Appl. Phys. **57**, 2617 (1985).
[22] H.-W. Fink, Phys. Scr. **38**, 260 (1988).
[23] J. Jersch, F. Demming, L. J. Hildenhagen, and K. Dickmann, Appl. Phys. A **66**, 29 (1998).
[24] A. Baltuška *et al.*, Nature (London) **421**, 611 (2003).
[25] G. G. Paulus *et al.*, Phys. Rev. Lett. **91**, 253004 (2003).
[26] A. Apolonski *et al.*, Phys. Rev. Lett. **92**, 073902 (2004).
[27] T. M. Fortier *et al.*, Phys. Rev. Lett. **92**, 147403 (2004).
[28] G. Sansone *et al.*, Phys. Rev. Lett. **92**, 113904 (2004).
[29] V. T. Binh, S. T. Purcell, N. Garcia, and J. Doglioni, Phys. Rev. Lett. **69**, 2527 (1992).
[30] M. L. Yu *et al.*, Phys. Rev. Lett. **77**, 1636 (1996).
[31] A. Zrenner *et al.*, Nature (London) **418**, 612 (2002).